

## Supporting Information

### Stimuli-Responsive Poly(ionic liquid) Nanoparticle for Controlled Drug Delivery

*Beibei Lu,<sup>a, b</sup> Gaixin Zhou,<sup>c, d</sup> Fan Xiao,<sup>e</sup> Qianjun He,<sup>c\*</sup> and Jiaheng Zhang<sup>a, b\*</sup>*

<sup>a</sup>State Key Laboratory of Advanced Welding and Joining, Harbin Institute of Technology, Shenzhen 518055, P. R. China.

<sup>b</sup>Research Centre of Printed Flexible Electronics, School of Materials Science and Engineering, Harbin Institute of Technology, Shenzhen 518055, P. R. China.

<sup>c</sup>Guangdong Provincial Key Laboratory of Biomedical Measurements and Ultrasound Imaging, National-Regional Key Technology Engineering Laboratory for Medical Ultrasound, School of Biomedical Engineering, Health Science Center, Shenzhen University, No. 1066 Xueyuan Road, Nanshan District, Shenzhen 518060, Guangdong, China.

<sup>d</sup>School of Biomedical Engineering and Informatics, Nanjing Medical University, Nanjing, 211166, P. R. China.

<sup>e</sup>School of Materials Science and Engineering, Harbin Institute of Technology, Nangang District, Harbin 150001, P. R. China.

E-mail: [zhangjiaheng@hit.edu.cn](mailto:zhangjiaheng@hit.edu.cn) (Jiaheng Zhang); [nanoflower@126.com](mailto:nanoflower@126.com) (Qianjun He)

## Table of Contents

<b>1. Materials and Characterization</b> .....	3
<b>Figure S1.</b> Synthesis of PIL-based block copolymer.....	5
<b>Figure S2.</b> Characterization of different polymers.....	6
<b>Figure S3.</b> Characterization of different polymers.....	7
<b>Table S1.</b> Characterization of polymer P1-P4.....	7
<b>Figure S4.</b> TEM image and DLS data.....	8
<b>Figure S5.</b> TEM image and DLS data.....	8
<b>Figure S6.</b> GPC chromatograms and Absorption spectra of P-3 before and after 10 days.....	9
<b>Table S2.</b> Characterization of P-1, P-2, P-3, P-4, and drug-loaded polymer nanoparticles.....	9
<b>Figure S7.</b> Zeta potentials .....	10
<b>Figure S8.</b> Illustration of the photo-response mechanism.....	10
<b>Figure S9.</b> TEM image (left) and DLS data (right).....	11
<b>Figure S10.</b> DOX released from P-1@DOX.....	11
<b>Figure S11.</b> CLSM images .....	12
<b>Figure S12.</b> CLSM images of MCF-7 and 4T1 cells. ....	12
<b>Figure S13.</b> Fluorescence intensity .....	13
<b>Figure S14.</b> Cell viability .....	13
<b>Table S3.</b> Calculated 50% inhibiting concentration (IC <sub>50</sub> ) .....	13
<b>Figure S15.</b> H&E stained histological images. ....	14
<b>References</b> .....	14

## 1. Materials and Characterization

*Materials:* 7-Hydroxycoumarin (PC), p-hydroxyazobenzene (AZO-OH), copper(I) bromide (CuBr), 1,4-dibromobutane, folic acid (FA), 2-hydroxyethyl methacrylate (HEMA), 2-(dimethylamino)ethyl methacrylate (DMAEMA), N-hydroxysuccinimide (NHS), N,N,N,N,N'-pentamethyldiethylene triamine (PMDETA), methacrylic acid (MAA), and 1-(3-Dimethylaminopropyl)-3-ethylcarbodiimide hydrochloride (EDC) were provided by Aladdin (Shanghai, China). Hyaluronic acid (HA; MW 4000 Da) was purchased from Shandong Freda Biopharm Co., Ltd (Shandong, China). Dimethyl sulfoxide (DMSO), dimethylformamide (DMF), and methanol were dried by refluxing over CaH<sub>2</sub> and distilled just before use. Cell counting kit-8 (CCK-8) and Annexin V-FITC apoptosis detection kit were purchased from Beyotime Biotechnology (Shanghai, China). Dulbecco's modified Eagle's medium (DMEM), fetal bovine serum (FBS), and pancreatic enzymes were obtained from Gibco (Grand Island, USA). 4% paraformaldehyde, 4, 6-diamidino-2-phenylindole (DAPI), and TritonX-100 were purchased from Solarbio (Beijing, China). Cyanine5.5 carboxylic acid (Cy5.5) was purchased from Seebio (Shanghai, China).

*Characterization:* The chemical structures of copolymers dispersed in DMSO-d<sub>6</sub> or CDCl<sub>3</sub> were analyzed by proton nuclear magnetic resonance (<sup>1</sup>H NMR) (Bruker Avance III 400, USA). Fourier transform infrared spectroscopy (FTIR) was performed using the IRTracer-100 spectrometer (Shimadzu, Japan) using KBr pellets. The molecular weight and molecular weight distribution of the copolymers were measured by gel permeation chromatography (GPC, Singapore) using a water Alliance e2695 gel permeation chromatography and DMF as the eluent. The morphology of the polymer nanoparticles was observed by transmission electron microscopy (TEM, 300 kV, FEI Tecnai G2 T12, Netherlands). The size and zeta potential of the nanoparticles were measured using a dynamic light scattering (DLS) method, by a Zetasizer (Nano ZS, Malvern, UK). The transmittance of the copolymer aqueous solution was recorded using an ultraviolet visible spectroscope (UV-Vis) (PerkinElmer, Lambda 365, USA).

Fluorimetric measurements of pyrene were conducted using the RF-6000 spectrofluorometer (Shimadzu, Japan), with excitation and emission set at 336 and 360 nm respectively, and a slit width of 10 nm. A small animal fluorescence imaging system (IVIS LuminaII+XGI-8, Caliper Life Science, USA) was used to observe the fluorescence distribution and metabolism of poly(ionic liquid)-based nanoparticles *in vivo*.

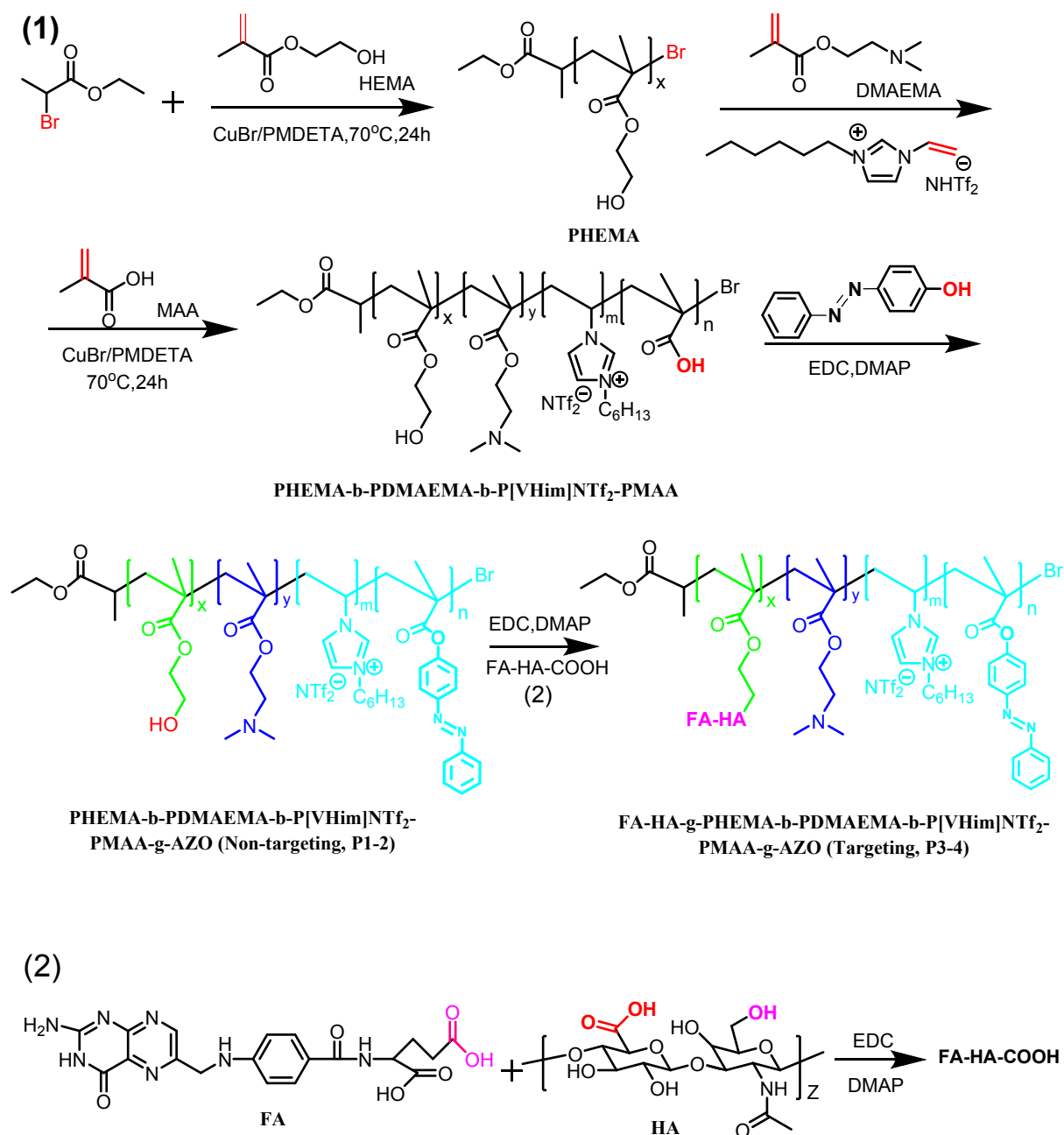


**Figure S1.** (1) Synthesis of PIL-based block copolymer PHEMA-b-PDMAEMA-b-P[VHim]NTf<sub>2</sub>-b-PMAA-g-AZO (P-1 and P-2) and FA-HA-g-PHEMA-b-PDMAEMA-b-P[VHim]NTf<sub>2</sub>-b-PMAA-g-AZO (P-3 and P-4) by ATRP. (2) Folic acid (FA) and hyaluronic acid (HA) form FA-HA-COOH through esterification.

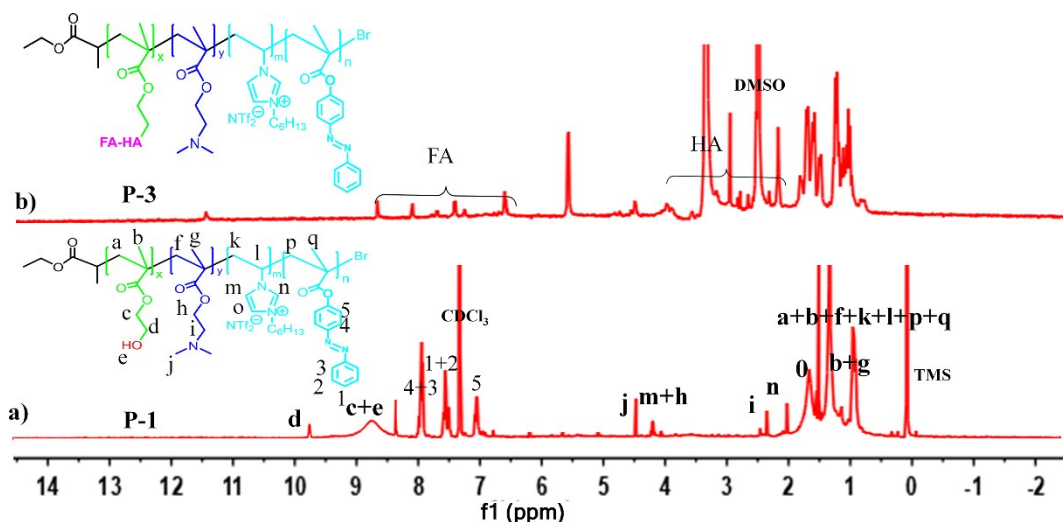


**Figure S2.** Characterization of different polymers.  $^1\text{H}$  NMR spectra of PHEMA-b-PDMAEMA-b-P[VHim]NTf<sub>2</sub>-b-PMAA-g-AZO (P-1, a) and FA-HA-g-PHEMA-b-PDMAEMA-b-P[VHim]NTf<sub>2</sub>-b-PMAA-g-AZO (P-3, a).

The chemical structures of PHEMA-b-PDMAEMA-b-P[VHim]NTf<sub>2</sub>-b-PMAA-g-AZO (P-1, a) and FA-HA-g-PHEMA-b-PDMAEMA-b-P[VHim]NTf<sub>2</sub>-b-PMAA-g-AZO (P-3, a) in DMSO-*d*<sub>6</sub> were analyzed by  $^1\text{H}$ -NMR spectra with a 400 MHz (Bruker AVANCE 400). (Figure S1 and S2). As shown in Figure S2a, the polymer spectra of AZO group,<sup>1</sup> the chemical shift of protons is approximate:  $\delta=7.94\text{--}7.96$  ppm (4, 3, ArH),  $\delta=7.46\text{--}7.55$  ppm (2, 1, ArH),  $\delta=7.77\text{--}7.82$  ppm (5, ArH). The peaks at  $\delta=0.50\text{--}2.00$  ppm (k and l,  $-\text{CH}_2\text{CCH}_2\text{CH}_3\text{COO}-$ ) and  $\delta=3.97$  ppm (c,  $-\text{OCH}_2\text{CH}_2\text{OH}$ ) due to the methyl and methylene peaks of PHEMA, respectively (Figure S2a). Which the peak of the methyl and methylene proton overlaps in PHEMA, PMAA, and PDMAEMA. Furthermore, Figure S2a shows that the peak at about  $\delta=0.91$  ppm is attributed to the  $-\text{CH}_3$  proton of the PDMAEMA block.<sup>2,3</sup> The overlap signal at  $\delta=4.10$  ppm,  $\delta=2.32$  ppm and  $\delta=1.61$  ppm is attributed to the protons of (h,  $-\text{COOCH}_2\text{CH}_2-$ ), (i,  $-\text{CH}_2\text{N}(\text{CH}_3)_2$ ), (j,  $-\text{CH}_2\text{N}(\text{CH}_3)_2$ ) in the PDMAEMA block, respectively. The synthesis of P[VHim]NTf<sub>2</sub> is indicated by the peak at  $\delta=9.60$  (n, pyridine-H) and  $\delta=8.54$  (m and o, pyridine-H are adjacent to the main chain) (Figure S2a).<sup>4</sup> Then, the  $^1\text{H}$ -NMR spectrum of HA shows the peak at  $\delta=4.50$  ppm, and  $\delta=3.30\text{--}3.90$  ppm in HA,  $\delta=2.10$  ppm (proton peak of acetyl group in HA) (Figure S2b).<sup>5</sup> It can be seen from Figure S2b that the characteristic peak of the nuclear magnetic resonance spectrum of FA shows that  $\delta=7.0\text{--}9.0$  ppm is the characteristic peak of FA.<sup>6</sup> Therefore, PIL-based block copolymer was successfully designed and synthesized.

In addition, it can be seen from the FTIR images in Figure S3a. Both  $^1\text{H}$  NMR and FTIR images results were indicated that the azobenzene group was successfully attached to the polymer (Figure S1). Gel permeation chromatography (GPC) further confirmed that PHEMA-

b-PDMAEMA-b-P[VHim]NTf<sub>2</sub>-b-PMAA-g-AZO (P-1 and P-2) and FA-HA-g-PHEMA-b-PDMAEMA-b-P[VHim]NTf<sub>2</sub>-b-PMAA-g-AZO (P-3 and P-4) polymer were successfully synthesized (Figure 3b; Table S1). It can be seen that the elution time of P-3 and P-4 shortened compared with the low molecular weight P-1 and P-2 polymer, indicating that the former has a higher Mn (Table S1). Further, P1-4 having different degrees of polymerization are shown in Table S1. Both copolymers showed a narrow polydispersity index (PDI).

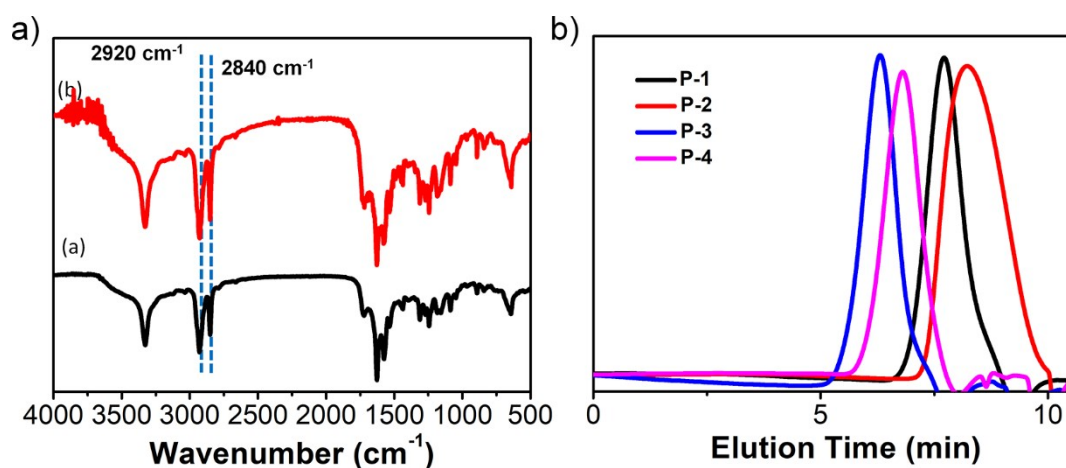


**Figure S3.** Characterization of different polymers. a) FTIR spectra of PHEMA-b-PDMAEMA-b-P[VHim]NTf<sub>2</sub>-b-PMAA-g-AZO (P-1, a) and FA-HA-g-PHEMA-b-PDMAEMA-b-P[VHim]NTf<sub>2</sub>-b-PMAA-g-AZO (P-3, b). b) GPC chromatograms of different polymers

**Table S1.** Characterization of polymer P1-P4

Sample <sup>(a)</sup>	$M_{n,NMR}^{(b)}$ (g mol <sup>-1</sup> )	$M_{n,GPC}^{(c)}$ (g mol <sup>-1</sup> )	PDI <sup>(c)</sup>
P-1	35854	36300	1.26
P-2	29360	28800	1.42
P-3	58732	59000	1.27
P-4	51259	50400	1.19

(a) Degree of theoretical polymerization. P-1: PHEMA<sub>30</sub>-b-PDMAEMA<sub>50</sub>-b-P[VHim]NTf<sub>2</sub>)<sub>40</sub>-b-PMAA<sub>40</sub>-g-AZO, P-2: PHEMA<sub>30</sub>-b-PDMAEMA<sub>50</sub>-b- P[VHim]NTf<sub>2</sub>)<sub>20</sub>-b-PMAA<sub>40</sub>-g-AZO, P-3: FA-HA-g-PHEMA<sub>30</sub>-b-PDMAEMA<sub>50</sub>-b- P[VHim]NTf<sub>2</sub>)<sub>40</sub>-b-PMAA<sub>40</sub>-g-AZO, P-4: FA-HA-g-PHEMA<sub>30</sub>-b-PDMAEMA<sub>50</sub>-b- P[VHim]NTf<sub>2</sub>)<sub>20</sub>-b-PMAA<sub>40</sub>-g-AZO.

(b) Calculated by <sup>1</sup>H NMR spectra.

(c) Determined by GPC with DMF as the eluent and polystyrene as the standard.

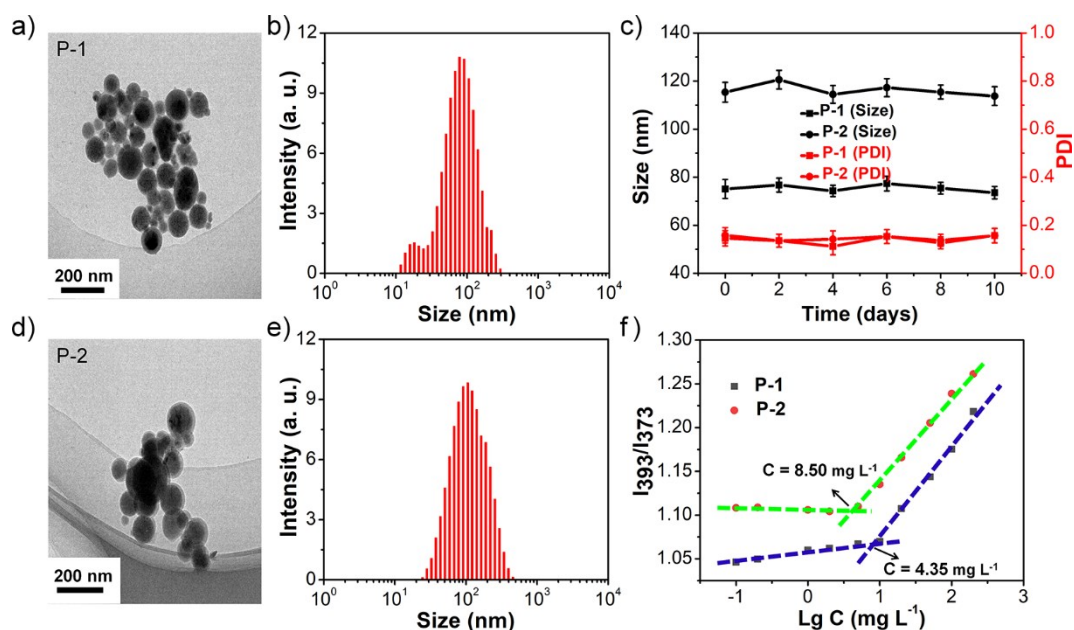


**Figure S4.** (a, d) TEM image and DLS data (b, e) of polymer nanoparticles. (c) Stabilities of size and PDI in aqueous solution. (f) Fluorescence intensity is a function of  $I_{393}/I_{373}$  as a function of polymer nanoparticle concentration in water.

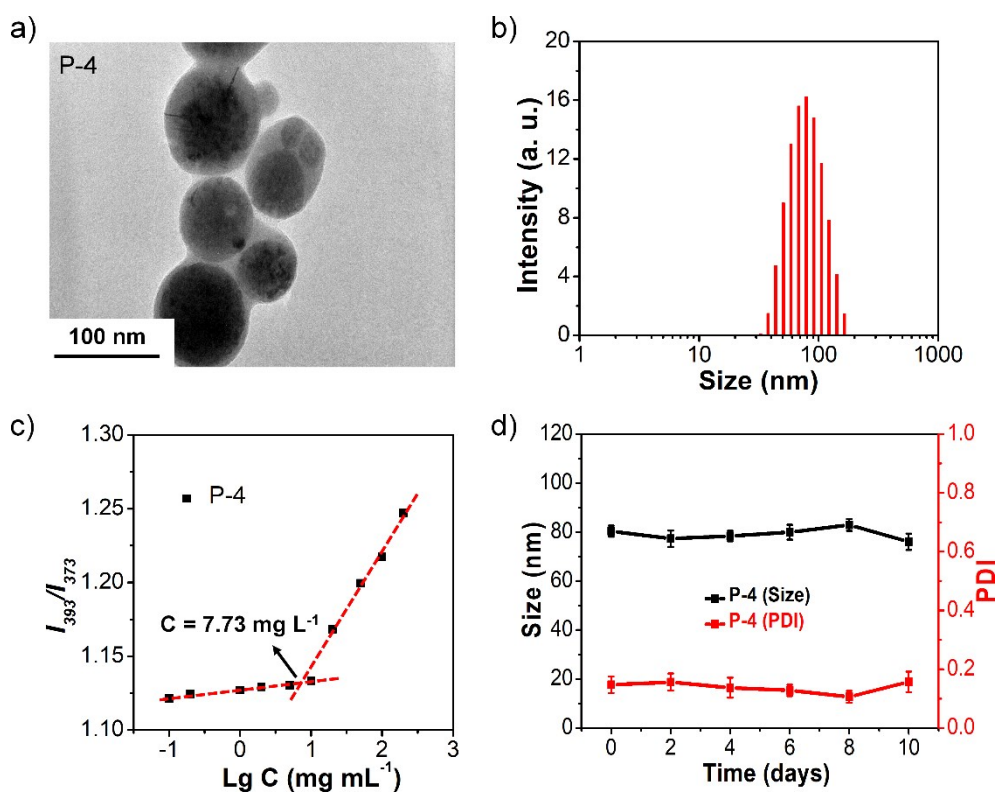


**Figure S5.** (a) TEM image and DLS data (b) of P-4. (c) Fluorescence intensity is a function of  $I_{393}/I_{373}$  as a function of polymer nanoparticle concentration in water. (d) Stabilities of size and PDI in aqueous solution.



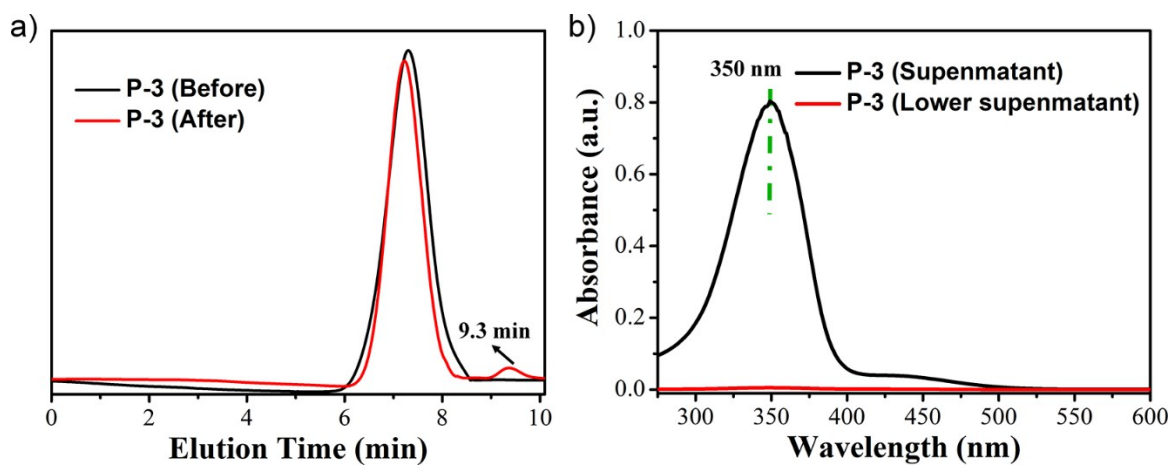


**Figure S6.** GPC chromatograms (a) and Absorption spectra (b) of P-3 before and after 10 days.

**Table S2.** Characterization of P-1, P-2, P-3, P-4, and drug-loaded polymer nanoparticles.

Sample	Size (nm)	PDI	Zeta Potential (mV)	DLC (%)	DEE (%)
P-1	75.08±3.96	0.146±0.019	8.12±1.67	/	/
P-1@DOX	121.87±3.27	0.142±0.020	-5.13±1.73	62.87±2.36	6.29±3.04
P-2	115.36±4.08	0.158±0.023	9.46±2.14	/	/
P-2@DOX	164.71±1.63	0.125±0.016	-5.47±1.48	46.08±2.57	4.61±2.42
P-3	38.16±1.63	0.081±0.025	7.02±1.51	/	/
P-3@DOX	54.53±3.26	0.137±0.031	-10.78±1.87	72.89±3.87	7.29±2.68
P-4	80.36±2.26	0.147±0.027	4.89±2.03	/	/
P-4@DOX	134.68±2.87	0.235±0.018	-8.25±2.94	65.06±2.94	6.51±2.39

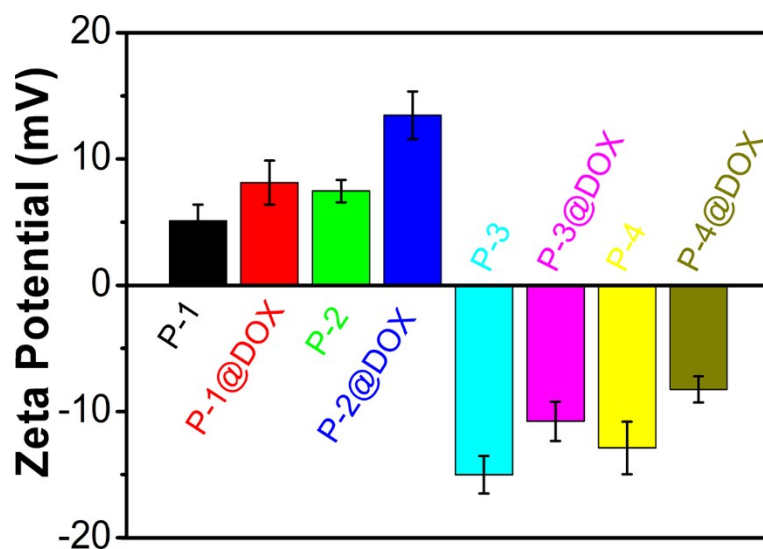


**Figure S7.** Zeta potentials of polymer nanoparticles and DOX-loaded polymer nanoparticles in aqueous media.

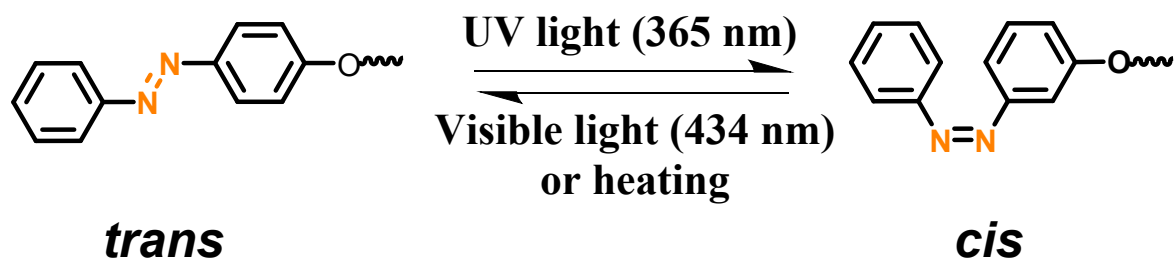


**Figure S8.** Illustration of the photo-response mechanism of PIL based azobenzene polymers (P1-4).

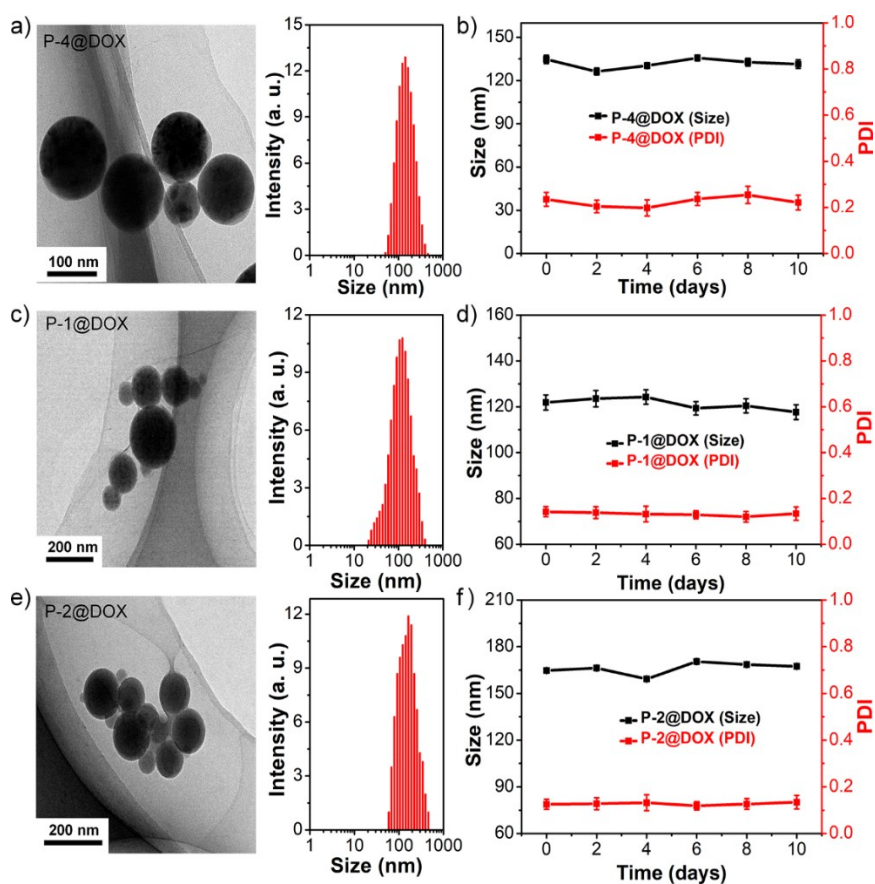


**Figure S9.** (a, c, e) TEM image (left) and DLS data (right) of DOX-loaded polymer nanoparticles. (b, d, f) Stabilities of size and PDI dispersed in aqueous solution (n=3).

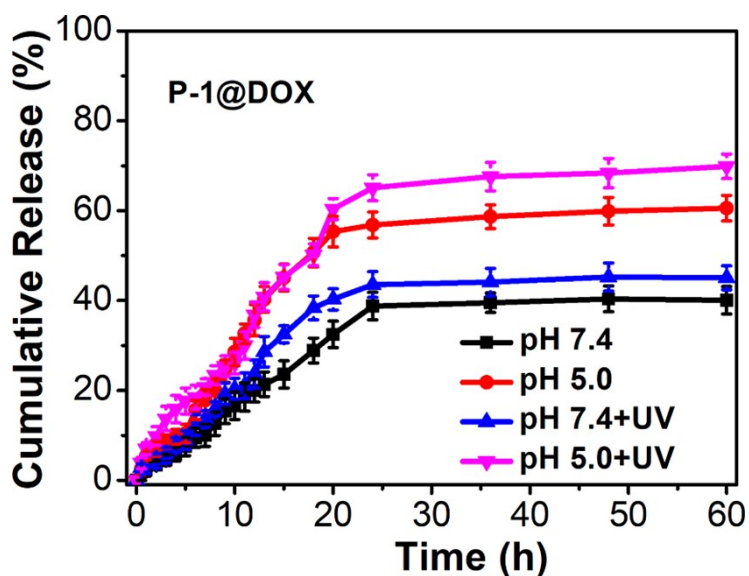


**Figure S10.** DOX released from P-1@DOX at pH 5.0 and 7.4 with or without UV (365 nm, 25 mW cm<sup>-2</sup>) irradiation.

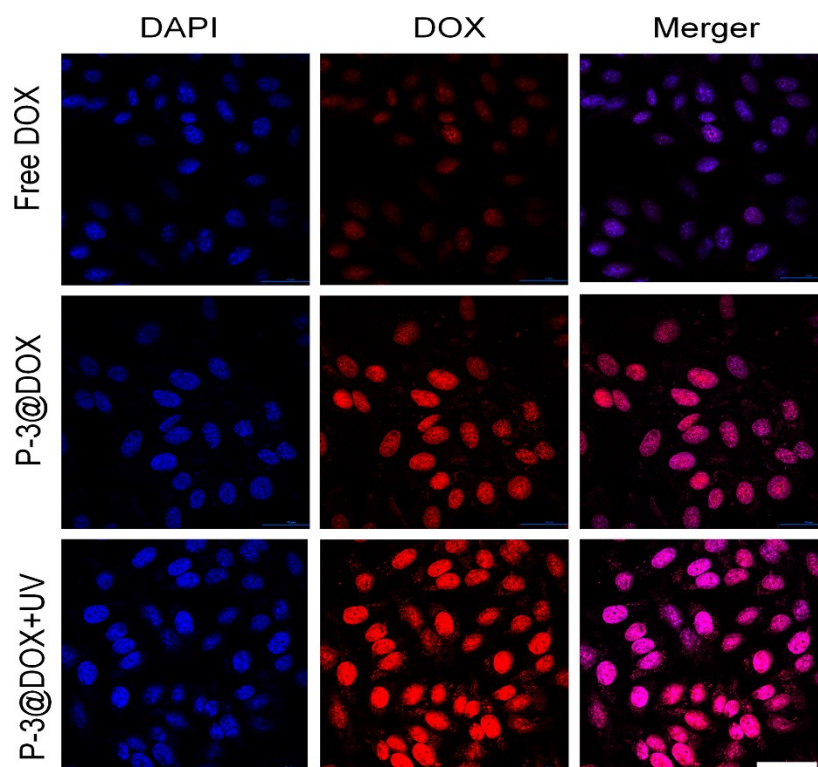


**Figure S11.** CLSM images of MCF-7 cells incubated with free DOX, P-3@DOX without or with UV irradiation (365 nm). DAPI stained nuclei blue, DOX fluorescence red, and merge purple. The DOX final concentration was  $10 \mu\text{g mL}^{-1}$ . (Scale bar:  $50 \mu\text{m}$ ).

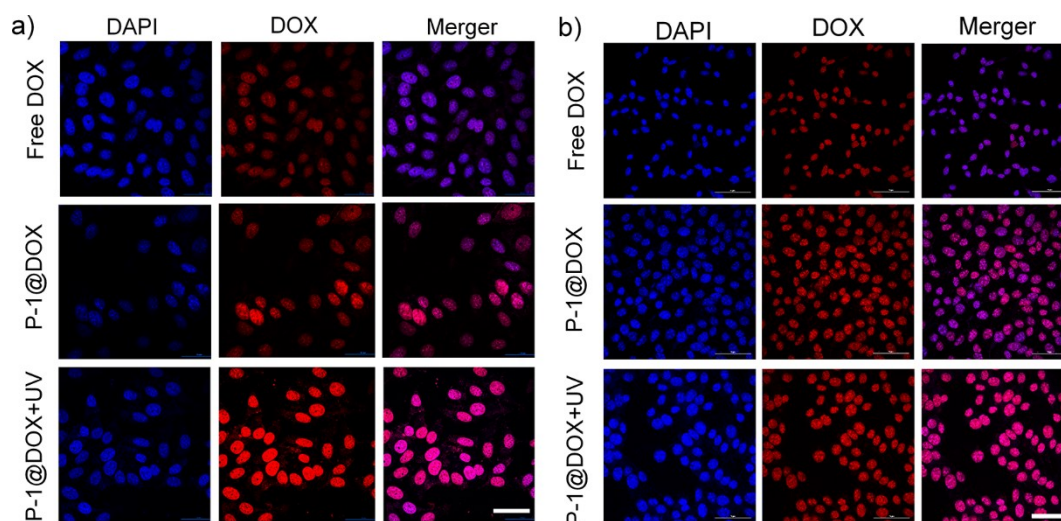


**Figure S12.** CLSM images of MCF-7 (a) and 4T1 (b) cells treated with free DOX, and P-1@DOX with or without UV light. DAPI-stained nuclei-blue, DOX fluorescence-red, and merger-purple. The DOX final concentration was  $10 \mu\text{g mL}^{-1}$ . (Scale bar:  $50 \mu\text{m}$ ).

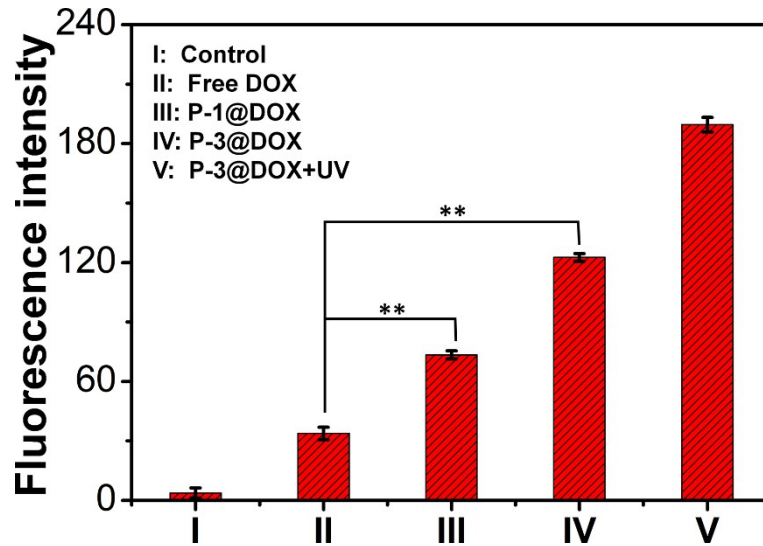


**Figure S13.** Fluorescence intensity of 4T1 (Figure 3c) cells incubated with the control group, free DOX, P-3@DOX, P-1@DOX, and P-1@DOX+UV nanoparticles for 4 h. (\*\*  $p < 0.01$ )

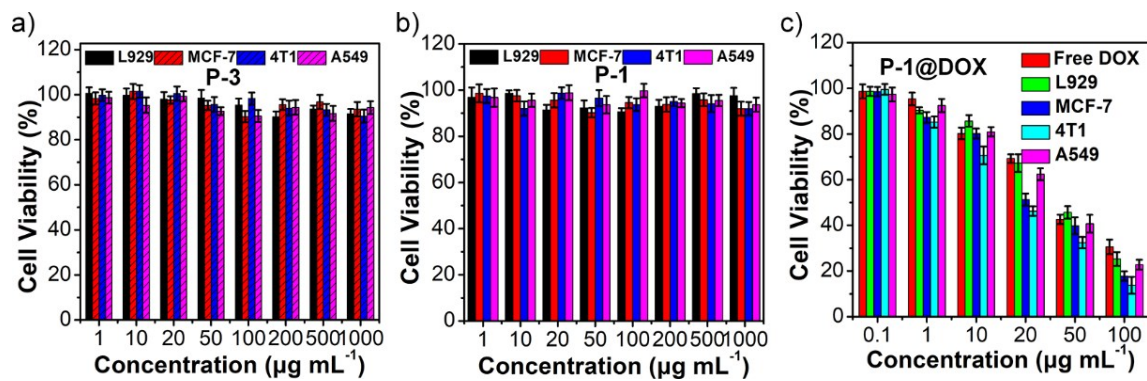


**Figure S14.** (a-b) Cell viability of L929, MCF7, 4T1, and A549 cells after incubation with P-1, P-3, and P-1@DOX nanoparticles for 24 h.

**Table S3.** Calculated 50% inhibiting concentration ( $IC_{50}$ ) of different formulations of DOX against L929, MCF-7, 4T1, and A549 cells.

Group	$IC_{50}$ ( $\mu\text{g mL}^{-1}$ )				
	Free DOX	L929	MCF-7	4T1	A549
P-1@DOX	44.32±2.65	41.89±2.76	23.49±2.59	18.95±2.58	37.21±3.17
P-3@DOX	32.53±2.06	27.81±1.98	18.28±2.17	15.11±1.88	25.76±2.47



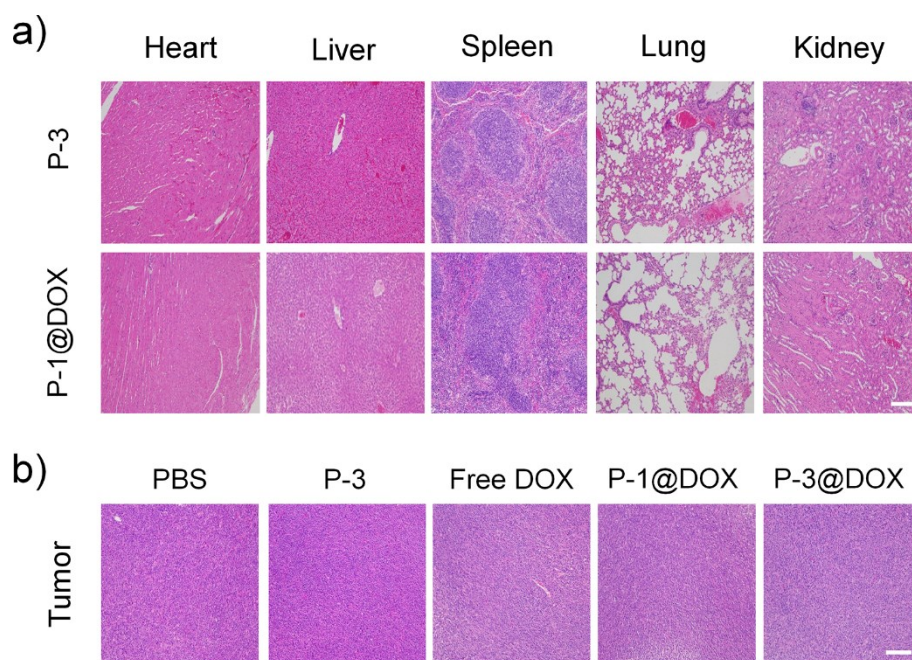


**Figure S15.** H&E stained histological images of tissue sections from major organs (a) and tumor (b) after 16 d of treatment with different groups. PBS was used as a control. Images were taken under a 100×objective. (Scale bar: 200 μm).

## References

1. S. Guan, Z. C. Deng, T. Y. Huang, W. Wen, Y. B. Zhao, A. H. Chen, *ACS Macro Lett.* 2019, **8**, 460-465.
2. M. J. Wang, K. W. He, J. L. Li, T. Shen, Y. Li, Y.T. Xu, C. H. Yuan, L. Z. Dai, *J. Biomater. Sci. Polym. Ed* 2020, **31**, 849-868.
3. H. Z. Deng, X. F. Zhao, J. J. Liu, J. H. Zhang, L. D. Deng, J. F. Liu, A. J. Dong, *Nanoscale*, 2016, **8**, 1437-1450.
4. J. Gravel, A. R. Schmitzer, *Supramol. Chem.* 2015, **27**, 364-371.
5. M. M. Sang, L. F. Han, R. J. Luo, W. Qu, F. Zheng, K. G. Zhang, F. L. Liu, J. W. Xue, W. Y. Liu, F. Feng, *Biomater. Sci.* 2019, **8**, 212-223.
6. F. Zhao, H. Yin, Z. X. Zhang, J. Li, *Biomacromolecules* 2013, **14**, 476-484.